International Journal of Modern Physics A
Vol. 30, No. 8 (2015) 1542003 (20 pages)

DOI: 10.1142/S0217751X15420038

Diffractive results from CDF

Konstantin Goulianos

Experimental High Energy Physics, The Rockefeller University,
1230 York Avenue, NY 10065, USA
dino@fnal.gov

Received 30 September 2014
Published 26 February 2015

We present a reference review of diffractive results from CDF for $\bar{p}p$ collisions at $\sqrt{s} =$ 540, 630, 1800, and 1960 GeV at the Tevatron, published in 19 PRL/PRD papers from 1994 to 2012. Both soft and hard diffractive results are included for single and/or double dissociation, central diffraction or double Pomeron exchange (where both the proton and antiproton remain intact), multi-gap diffraction (a combination of single and double dissociation), elastic scattering, and the total cross-section, which through the optical theorem is related to the imaginary part of the forward elastic scattering amplitude. In each review, we include the comparisons made by CDF with theoretical predictions.

Keywords: Diffraction; CDF; Tevatron.

PACS numbers: 12.40.Nn, 13.85.Dz, 25.43.+t

1. Introduction

We present a reference review of the diffractive results published by the CDF Collaboration (CDF) using data collected during Tevatron Collider operations.

The order of presentation of the papers in this review does not follow the chronological order of publication, but is rather organized by the class of physics processes studied. This format has been chosen in order to provide a better understanding of the interrelationships between papers in the same physics class.

The review addresses the following physics processes:

I Elastic and Total Cross-Sections;
II Soft Diffraction;
III Hard Diffraction;

  A Single/Double Diffraction,
  B Hard Central Diffraction/Double Pomeron Exchange (DPE),
  C Rapidity Gaps Between Jets.

For each paper, we present a brief description of the important findings and their physics significance, and in most cases we include figures showing the key results.

I. *Elastic and total cross-sections*

(1) Measurement of small angle antiproton–proton elastic scattering at $\sqrt{s} = 546$ and 1800 GeV (1994).[1]
(2) Measurement of the antiproton–proton total cross-section at $\sqrt{s} = 546$ and 1800 GeV (1994).[2]

II. *Soft diffraction*

(3) Measurement of $\bar{p}p$ single diffraction dissociation at $\sqrt{s} = 546$ and 1800 GeV (1994).[3]
(4) Double Diffraction Dissociation at the Fermilab Tevatron Collider (1995).[12]
(5) Central Pseudorapidity Gaps in Events with a Leading Antiproton at the Fermilab Tevatron $\bar{p}p$ Collider (2003).[15]
(6) Inclusive Double Pomeron Exchange at the Fermilab Tevatron $\bar{p}p$ Collider (2004).[16]

III. *Hard diffraction*

A. *Hard single/double diffraction*

(7) Observation of Diffractive W-Boson Production at the Fermilab Tevatron (1997).[5]
(8) Measurement of Diffractive Dijet Production at the Fermilab Tevatron (1997).[6]
(9) Observation of Diffractive b-Quark Production at the Fermilab Tevatron (2000).[9]
(10) Diffractive Dijets with a Leading Antiproton in pbar-p Collisions at $\sqrt{s} =$ 1800 GeV (2000).[10]
(11) Observation of Diffractive J/ψ Production at the Fermilab Tevatron (2001).[13]
(12) Diffractive Dijet Production at $\sqrt{s} = 630$ and 1800 GeV at the Fermilab Tevatron (2002).[14]
(13) Diffractive W and Z Production at the Fermilab Tevatron (2010).[18]
(14) Diffractive Dijet Production in $\bar{p}p$ Collisions at $\sqrt{s} = 1.96$ TeV (2012).[19]

B. *Hard central diffraction/double Pomeron exchange*

(15) Dijet Production by Double Pomeron Exchange at the Fermilab Tevatron (2000).[11]
(16) Observation of Exclusive Dijet Production at the Fermilab Tevatron $p\bar{p}$ Collider (2008).[17]

C. *Rapidity gaps between jets*

(17) Observation of Rapidity Gaps in $\bar{p}p$ Collisions at 1.8 TeV (1995).[4]
(18) Dijet Production by Color-Singlet Exchange at the Fermilab Tevatron (1998).[7]
(19) Events with a Rapidity Gap between Jets in $\bar{p}p$ Collisions at $\sqrt{s} = 630\,\mathrm{GeV}$ (1998).[8]

2. Reference Reviews by Paper

2.1. *I* (1): *Measurement of small angle antiproton–proton elastic scattering at* $\sqrt{s} = 546$ *and* 1800 GeV (1994)[1]

Antiproton–proton elastic scattering was measured at energies of $\sqrt{s} = 546$ and 1800 GeV in the range of four-momentum transfer squared $0.025 < -t < 0.29\,\mathrm{GeV}^2$. The data are well described by the exponential form e^{bt} with a slope $b = 15.28 \pm 0.58\,(16.98 \pm 0.25\,\mathrm{GeV}^{-2})$ at $\sqrt{s} = 1800\,(546)\,\mathrm{GeV}$. The measured elastic scattering cross-sections are, respectively, $\sigma_{\mathrm{el}} = 12.87 \pm 0.30$ and $19.70 \pm 0.75\,\mathrm{mb}$.

It is recommended that this paper be read together with the papers of the antiproton–proton total cross-section, *I* (2), and single diffraction dissociation, *I* (3), as there are common analysis issues and cross-references among all three papers.

2.2. *I* (2): *Measurement of the antiproton–proton total cross-section at* $\sqrt{s} = 546$ *and* 1800 GeV (1994)[2]

In this paper, CDF reports a measurement of the proton–antiproton total cross-section σ_T at energies of $\sqrt{s} = 546$ and 1800 GeV. Using the luminosity-independent method, values of $\sigma_T = 61.26 \pm 0.93\,\mathrm{mb}$ at $\sqrt{s} = 546\,\mathrm{GeV}$ and $80.03 \pm 0.24\,\mathrm{mb}$ at 1800 GeV were obtained. In this energy range, the ratio $\sigma_{\mathrm{el}}/\sigma_T$ increases from 0.201 ± 0.002 to 0.246 ± 0.004.

In order to understand the data analysis that led to the results presented in this paper, one should also read the papers of antiproton–proton elastic scattering, *I* (1), and single diffraction dissociation, *I* (3), as there are common issues and cross-references among all these three papers.

2.3. *I* (3): *Measurement of* $\bar{p}p$ *single diffraction dissociation at* $\sqrt{s} = 546$ *and* 1800 GeV (1994)[3]

Results form measurements of the diffraction dissociation differential cross-section $d^2\sigma_{\mathrm{SD}}/dM^2dt$ for $\bar{p}p \to \bar{p}X$ at $\sqrt{s} = 546$ and 1800 GeV, $M^2/s < 2$, and $0 \leq -t \leq 0.4\,\mathrm{GeV}^2$ are reported. The results are compared to theoretical predictions and to extrapolations from experimental results at lower energies.

This paper should be consulted together with the papers of the measurements of the antiproton–proton elastic scattering, *I* (1), and the total cross-section, *I* (2), as there are common data analysis issues among them, the details of which are not presented in each one paper.

2.4. *II* (4): *Double diffraction dissociation at the Fermilab Tevatron Collider* (1995)[12]

Results are presented from a measurement of double diffraction dissociation in $\bar{p}p$ collisions at the Fermilab Tevatron collider. The production cross-section for events with a central pseudorapidity gap of width $\Delta\eta^0 > 3$ (overlapping $\eta = 0$) is found to be $4.43 \pm 0.02\,(\text{stat}) \pm 1.18\,(\text{syst})$ mb $[3.42 \pm 0.01\,(\text{stat}) \pm 1.09\,(\text{syst})$ mb$]$ at $\sqrt{s} = 1800$ [630] GeV. The results are compared with previous measurements and with predictions based on Regge theory and factorization.

Figure 1 is a schematic diagram of the double diffraction dissociation process. In Fig. 2, the total diffraction dissociation cross-sections $\sigma_{\rm DD}$ (mb) for $\Delta\eta > 3.0$, extrapolated from the measured regions to $\Delta\eta > 3.0$, are compared to the UA5 adjusted results and to Renormalized-Gap (RENORM) predictions (see caption).

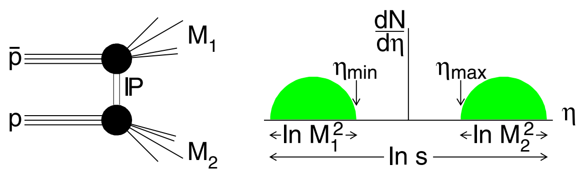

Fig. 1. Schematic diagram and event topology in pseudorapidity space of a double diffractive $\bar{p}p$ interaction.

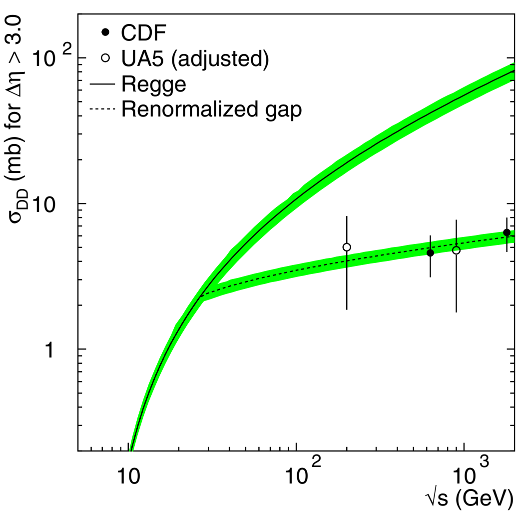

Fig. 2. The total double diffractive cross-section for $p(\bar{p})+p \to X_1+X_2$ versus $\sqrt{s}$ compared with predictions from Regge theory based on the triple-Pomeron amplitude and factorization (solid curve), and from the renormalized gap probability model [K. Goulianos, arXiv:hep-ph/0203141] (dashed curve).

2.5. *II* (5): *Central pseudorapidity gaps in events with a leading antiproton at the Fermilab Tevatron $\bar{p}p$ Collider* (2003)[15]

The fraction of events with a large pseudorapidity gap $\Delta\eta$ within the pseudorapidity region available to the proton dissociation products X in $\bar{p} + p \to \bar{p} + X$ is presented. For a final state $\bar{p}$ of fractional momentum loss $\xi_{\bar{p}}$ and four-momentum transfer squared $t_{\bar{p}}$ within $0.06 < \xi_{\bar{p}} < 0.09$ and $|t_{\bar{p}}| < 1.0$ [0.2] GeV^2 at $\sqrt{s} = 1800$ [630] GeV, the fraction of events with $\Delta\eta > 3$ is found to be 0.246 ± 0.001 (stat) $\pm$ 0.042 (syst) [0.184 ± 0.001 (stat) $\pm$ 0.043 (syst)]. They are compared with gap fractions measured in minimum bias $\bar{p}p$ collisions and with theoretical expectations.

Figure 3 is a schematic diagram of the central pseudorapidity gap process. In Fig. 4, the ratios of the measured cross-sections are compared to Regge and Renormalized-Gap (RENORM) predictions [K. Goulianos, arXiv:hep-ph/0203141].

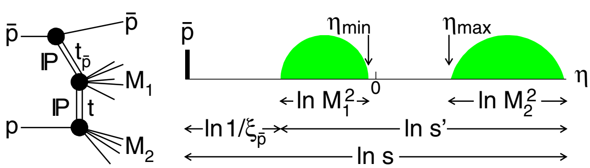

Fig. 3. Schematic diagram and event topology in pseudorapidity space of a SDD (single diffraction plus gap) interaction, $\bar{p}+p \to \bar{p}+\mathrm{GAP}_{\bar{p}}+M_1+\mathrm{GAP}+M_2$, with a leading outgoing antiproton of fractional momentum loss $\xi_{\bar{p}}$, associated with a pseudorapidity gap $\Delta\eta_{\bar{p}} = \ln\frac{1}{\xi_{\bar{p}}}$, and a gap within the region of η spanned by $\ln s' = \ln s - \ln\frac{1}{\xi_{\bar{p}}}$.

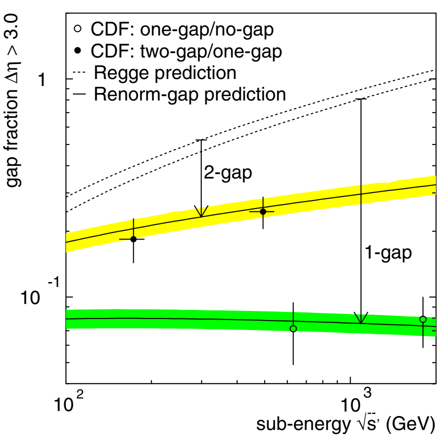

Fig. 4. Ratios of SDD (single-diffraction plus gap) to single-diffractive rates (filled circles) and double-diffractive to total cross-sections (open circles) as a function of the collision energy of the sub-process, Pomeron-proton and $\bar{p}p$, respectively. The uncertainties are mainly due to systematic effects, which are highly correlated among all four data points. The dashed lines are predictions from Regge theory and the solid lines from the renormalized gap probability model [K. Goulianos, arXiv:hep-ph/0203141].

2.6. *II* (6): *Inclusive double-pomeron exchange at the Fermilab Tevatron $\bar{p}p$ Collider* (2004)[16]

A study of the reaction $\bar{p}+p \to \bar{p}' + X + Y$ at $\sqrt{s} = 1800\,\mathrm{GeV}$ is presented, where $\bar{p}'$ is detected in a RPS and Y is a proton or proton dissociation system of mass-squared $M_Y^2 \lesssim 8\,\mathrm{GeV}^2$. In events with a $\bar{p}'$ of fractional momentum loss $0.035 < \xi_{\bar{p}} < 0.095$ and four-momentum transfer squared $|t_{\bar{p}}| < 1.0\,\mathrm{GeV}^2$, the fractional momentum loss ξ_p^X of the proton or system Y, evaluated from the momenta of the particles comprising X, behaves as $\approx 1/\xi_p^X$ at small ξ_p^X, as expected for DPE. The fraction of events with $\xi_p^X < 0.02$ is $0.194 \pm 0.001\,(\mathrm{stat}) \pm 0.012\,(\mathrm{syst})$.

Schematic diagrams of event topologies for SD and DPE are shown in Fig. 5, and a histogram of the measured differential event spectrum versus $\xi_{\bar{p}}^X$ is displayed and compared to Renormalized-Gap (RENORM) MC predictions in Fig. 6.

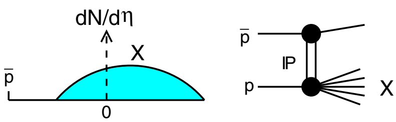

(a)

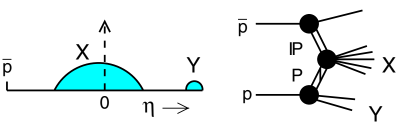

(b)

Fig. 5. Schematic diagrams and event topologies for (a) single diffraction, $\bar{p}+p \to \bar{p}+X$, and (b) DPE, $\bar{p}+p \to \bar{p}+X+Y$; the filled areas are η regions of particle production.

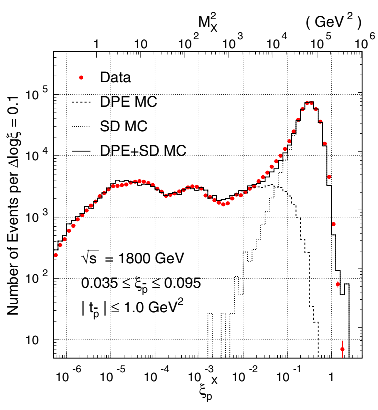

Fig. 6. Distribution of proton fractional momentum loss ξ_p^X, measured from calorimeter and beam–beam counter information, for events with a leading $\bar{p}$ of $0.035 < \xi_{\bar{p}}^{\mathrm{RPS}} < 0.095$ and $|t_{\bar{p}}| < 1.0\,\mathrm{GeV}^2$; the curves are from a Monte Carlo simulation of SD (dotted), DPE (dashed) and total (solid) contributions normalized to the data points; the DPE events were generated for $\xi_p < 0.1$.

2.7. *III A* (7): *Observation of diffractive W-boson production at the Fermilab Tevatron* (1997)[5]

This paper reports the first observation of diffractively produced W bosons. In a sample of $W \to e\nu$ events produced in $p\bar{p}$ collisions at $\sqrt{s} = 1.8\,\mathrm{TeV}$, an excess of events with a forward rapidity gap is found, which is attributed to diffraction. The probability that this excess is consistent with nondiffractive production is 1.1×10^{-4} (3.8σ). The relatively low fraction of W + Jet events observed within this excess implies that mainly quarks from the pomeron, which mediates diffraction, participate in W production. The diffractive to nondiffractive W production ratio is found to be $R_W = (1.15 \pm 0.55)\%$.

Quote from paper: "We searched for a diffractive W signal by analyzing the correlations between the η of the electron, η_e, or the sign of its charge, C_e, and the multiplicity of one or the other of the Beam–Beam Counters (BBCs). Each event enters into two distributions, one with $\eta_e \cdot \eta_{\mathrm{BBC}} < 0$ (angle-correlated) or $C_e \cdot \eta_{\mathrm{BBC}} < 0$ (charge-correlated), and the other with $\eta_e \cdot \eta_{\mathrm{BBC}} > 0$ (angle-anticorrelated) or $C_e \cdot \eta_{\mathrm{BBC}} > 0$ (charge-anticorrelated). A doubly-correlated (anticorrelated) distribution is the BBC multiplicity distribution for events with $\eta_e \cdot C_e > 0$ and $\eta_e \cdot \eta_{\mathrm{BBC}} < 0$ ($\eta_e \cdot \eta_{\mathrm{BBC}} > 0$)."

The main result reported in this paper, indicating a gap signal in the diffractive to nondiffractive event ratio, is shown in Fig. 7.

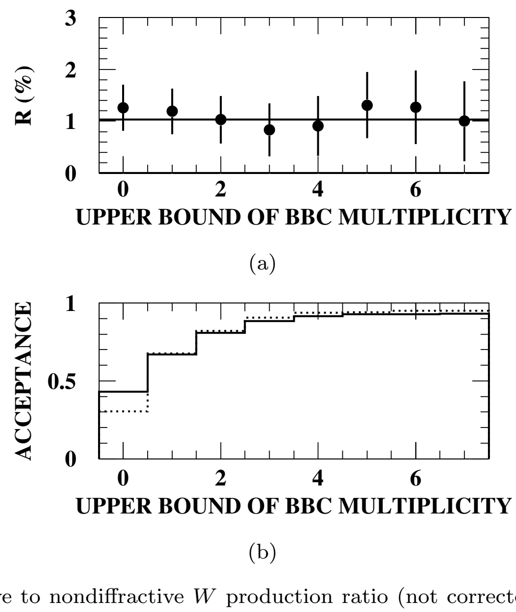

Fig. 7. (a) Diffractive to nondiffractive W production ratio (not corrected for BBC occupancy or one-vertex cut efficiency) as a function of upper bound BBC multiplicity. The solid line passes through the $N_B = 2$ point, which we use as our result; (b) gap-acceptance for angle-gap and charge-gap doubly correlated (solid) and anticorrelated (dashed) diffractive events with an electron within $|\eta| < 1.1$.

2.8. *III A* (8): *Measurement of diffractive dijet production at the Fermilab Tevatron* (1997)[6]

The observation and measurement of the rate of diffractive dijet production at the Fermilab Tevatron $\bar{p}p$ collider at $\sqrt{s} = 1.8\,\text{TeV}$ is reported. In events with two jets of $E_T > 20\,\text{GeV}$, $1.8 < |\eta| < 3.5$ and $\eta_1\eta_2 > 0$, it is found that the diffractive to nondiffractive production ratio is $R_{JJ} = [0.75 \pm 0.05\,(\text{stat}) \pm 0.09\,(\text{syst})]\%$. By comparing this result, in combination with the measured rate for diffractive W boson production reported previously, with predictions based on a hard partonic pomeron structure, the Pomeron gluon fraction is determined to be $f_g = 0.7 \pm 0.2$.

Figures 8 and 9 show the method of extracting the signal and the physics significance of the results, respectively.

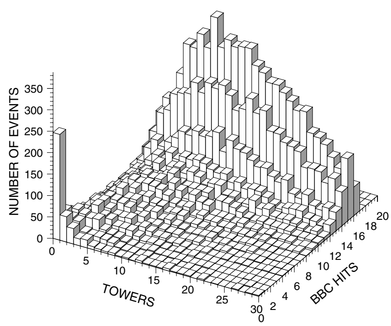

Fig. 8. Beam–beam counter multiplicity (BBC hits) versus forward calorimeter tower multiplicity in the pseudorapidity regions $3.2 < |\eta_{(\text{BBC})}| < 5.9$ and $2.4 < |\eta_{(\text{tower})}| < 4.2$ opposite the dijet system.

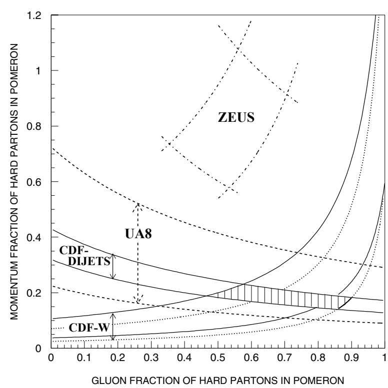

Fig. 9. Momentum fraction versus gluon fraction of hard partons in the pomeron evaluated by comparing measured diffractive rates with Monte Carlo predictions based on the standard pomeron flux and assuming that only hard pomeron partons participate in the diffractive processes considered. Results are shown for ZEUS (dashed–dotted), UA8 (dashed) and the CDF-dijet and CDF-W measurements. The CDF-W result is shown for two (dotted) or three (solid) light quark flavors in the pomeron. The shaded region is used in the text to extract the quark to gluon fraction of the pomeron and the standard flux discrepancy factor.

2.9. *III A* (9): *Observation of diffractive b-quark production at the Fermilab Tevatron* (2000)[9]

In this paper, CDF reports a measurement of the fraction of b-quarks produced diffractively in $\bar{p}p$ collisions at $\sqrt{s} = 1.8\,\text{TeV}$. Diffraction is identified by the absence of particles in a forward pseudorapidity region. From events with an electron of transverse momentum $9.5 < p_T^e < 20\,\text{GeV}$ within the pseudorapidity region $|\eta| < 1.1$, the ratio of diffractive to total b-quark production rates is found to be $R_{\bar{b}b} = [0.62 \pm 0.19\,(\text{stat}) \mp 0.16\,(\text{syst})]$. This result is comparable in magnitude to corresponding ratios for W and dijet production, but significantly lower than expectations based on factorization.

In Fig. 10, it is seen that this measurement, along with the diffractive dijet[6] and W[5] production measurements, restricts the gluon fraction of the Pomeron to a region compatible with that of the ZEUS result determined from ep collisions at HERA [M. Derrik *et al.*, *Z. Phys. C* **68**, 569 (1995)]. The value obtained by CDF is $f_g^{\text{CDF}} = 0.54^{+0.16}_{-0.14}$.

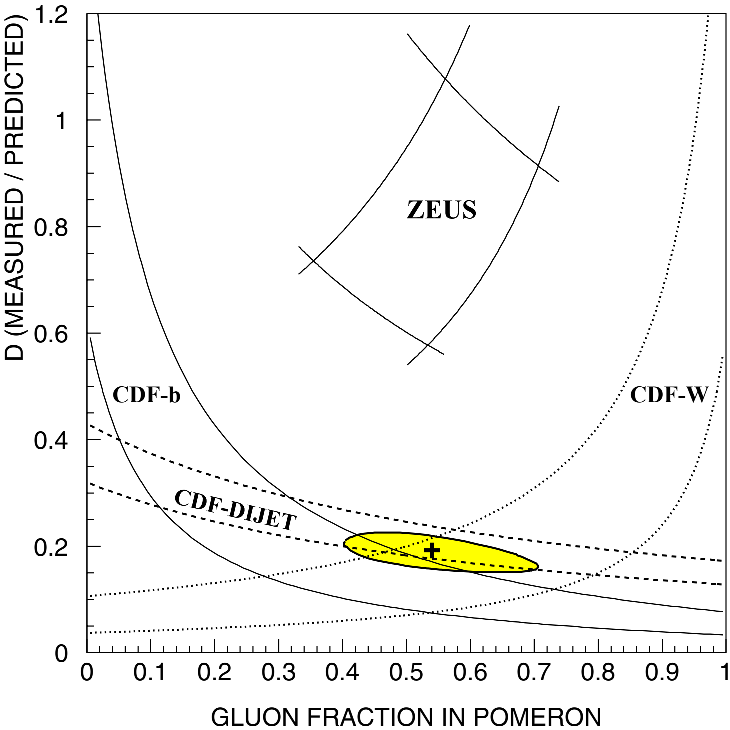

Fig. 10. The ratio, D, of measured to predicted diffractive rates as a function of the gluon content of the Pomeron. The predictions are from POMPYT using the standard Pomeron flux and a hard Pomeron structure. The CDF-W curves were calculated assuming a three-flavor quark structure for the Pomeron. The black cross and shaded ellipse are the best fit and 1σ contour of a least square two-parameter fit to the three CDF results.

2.10. *III A (10): Diffractive dijets with a leading antiproton in pbar-p collisions at $\sqrt{s} = 1800\,\mathrm{GeV}$ (2000)*[10]

Results are reported from a study of events with a leading antiproton of beam momentum fraction $0.905 < x_F < 0.965$ and four-momentum transfer squared $|t| < 3\,\mathrm{GeV}^2$ produced in $\bar{p}p$ collisions at $\sqrt{s} = 1800\,\mathrm{GeV}$ at the Fermilab Tevatron collider. Approximately 2% of the events contain two jets of transverse energy $E_T^{jet} > 7\,\mathrm{GeV}$. Using the dijet events, the diffractive structure function of the antiproton is evaluated and compared with expectations based on results obtained in diffractive deep inelastic scattering experiments at the DESY *ep* collider HERA.

The main result presented in this paper is the measurement of the diffractive structure function $\tilde{F}_{jj}^{D}(\beta)$, which is shown in Fig. 11 along with two H1 measurements, H1 fit-2 and H1 fit-3 [T. Ahmed *et al.*, *Phys. Lett. B* **348**, 681 (1995); C. Adloff *et al.*, *Z. Phys. C* **76**, 613 (1997)].

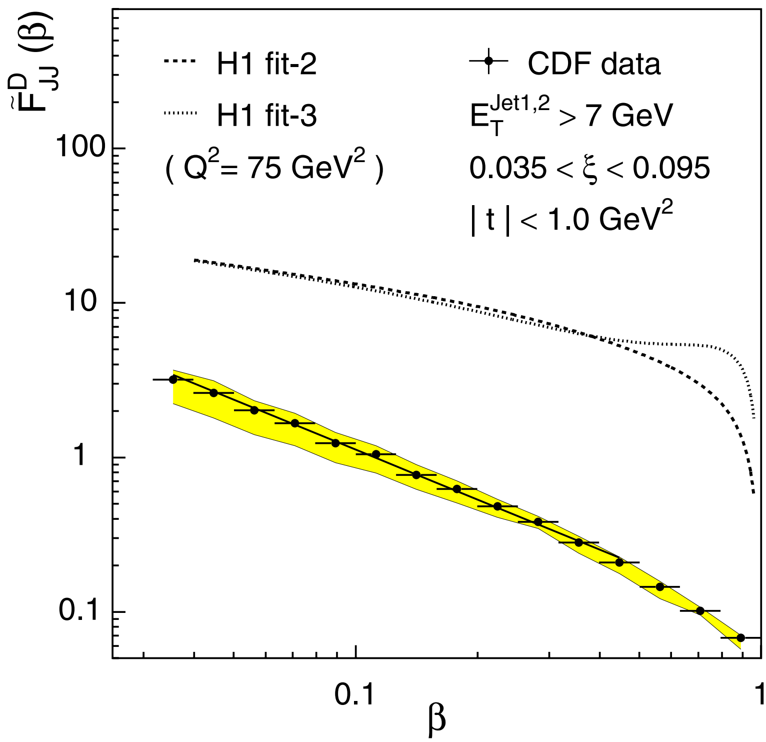

Fig. 11. Data β distribution (points) compared with expectations from the parton densities of the proton extracted from diffractive deep inelastic scattering by the H1 Collaboration. The straight line is a fit to the data of the form β^{-n}. The lower (upper) boundary of the filled band represents the data distribution obtained by using only the two leading jets (up to four jets of $E_T > 5\,\mathrm{GeV}$) in evaluating β. The dashed (dotted) lines are expectations from the H1 fit 2 (fit 3). The systematic uncertainty in the normalization of the data is ±25%.

2.11. *III A* (11): *Observation of diffractive J/ψ production at the Fermilab Tevatron* (2001)[13]

In this paper, CDF reports the first observation of diffractive $j/\psi(\to \mu^+\mu^-)$ production in $\bar{p}p$ collisions at $\sqrt{s} = 1.8\,\text{TeV}$. Diffractive events are identified by their rapidity gap signature. In a sample of events with two muons of transverse momentum $p_T^\mu > 2\,\text{GeV}/c$ within the pseudorapidity region $|\eta| < 1.0$, the ratio of diffractive to total J/ψ production rates is found to be $R_{J/\psi} = [1.45 \pm 0.25]\%$. The ratio $R_{j/\psi}(x)$ is presented as a function of x-Bjorken. By combining it with the previously CDF measured corresponding ratio $R_{jj}(x)$ for diffractive dijet production, a value of 0.59 ± 0.15 is extracted for the gluon fraction of the diffractive structure function of the proton.

Figure 12 shows the ratio of SD to ND events versus x-Bjotken. Integrating the x_{bj} distributions for R_{jj} and $R_{J/\psi}$ in the region $0.004 \leq x \leq 0.01$ (kinematic boundaries for full acceptance) yields $[R_{jj}(x)/R_{J/\psi}(x)]_{\text{exp}} = 1.17 \pm 0.27\,(\text{stat})$. The gluon fraction of the diffractive structure function of the (anti)proton is found to be $f_g^D = 0.9 \pm 0.14\,(\text{stat}) \pm 0.06\,(\text{syst})$, which is consistent with the value 0.54 ± 0.15 obtained by combining the results of diffractive W, dijet, and b-quark production, as discussed in Sec. 2.9.

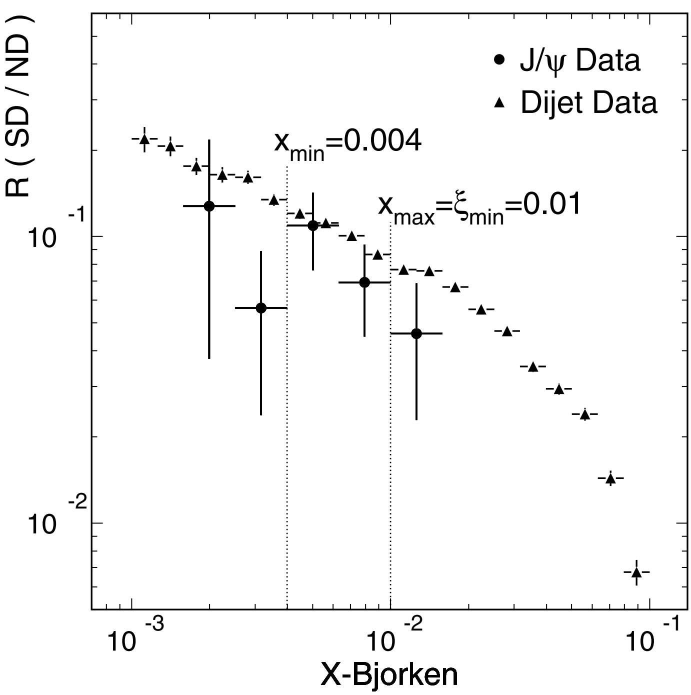

Fig. 12. Ratios of diffractive to total J/ψ (circles) and dijet (triangles) rates per unit $\xi_p(\xi_{\bar{p}})$ as a function of x-Bjorken of the struck parton of the $p(\bar{p})$ adjacent to the rapidity gap.

2.12. *III A* (12): *Diffractive dijet production at* $\sqrt{s} = 630$ *and* 1800 GeV *at the Fermilab Tevatron* (2002)[14]

The subject of this paper is the measurement of the diffractive structure function F_{jj}^D of the antiproton, obtained from a study of dijet events produced in association with a leading antiproton in $\bar{p}p$ collisions at $\sqrt{s} = 630\,\text{GeV}$ at the Fermilab Tevatron. The ratio of F_{jj}^D at $\sqrt{s} = 630\,\text{GeV}$ to F_{jj}^D obtained from a similar measurement at $\sqrt{s} = 1800\,\text{GeV}$ is compared with expectations from QCD factorization and other theoretical predictions. Also reported in this paper is a measurement of the ξ (x-Pomeron) and β (x of parton in Pomeron) dependence of F_{jj}^D at $\sqrt{s} = 1800\,\text{GeV}$. In the region $0.035 < \xi < 0.095$, $|t| < 1\,\text{GeV}^2$, and $\beta < 0.5$, $F_{jj}^D(\beta, \xi)$ is found to be of the form $\beta^{-1.0\pm0.1}\xi^{-0.9\pm0.1}$, which obeys β-ξ factorization.

The results of this measurement are summarized in Fig. 13, which displays on (left) the diffractive structure functions $\tilde{F}_{jj}^D$ versus β at $\sqrt{s} = 530$ and 1800 GeV, and on (right) the ξ dependence (fractional momentum loss of the leading $\bar{p}$) of the parameters that characterize $\tilde{F}_{jj}^D$ (see figure caption). The diffractive structure functions at the two energies are similar, except for an overall suppression at $\sqrt{s} = 1800\,\text{GeV}$ relative to 600 GeV.

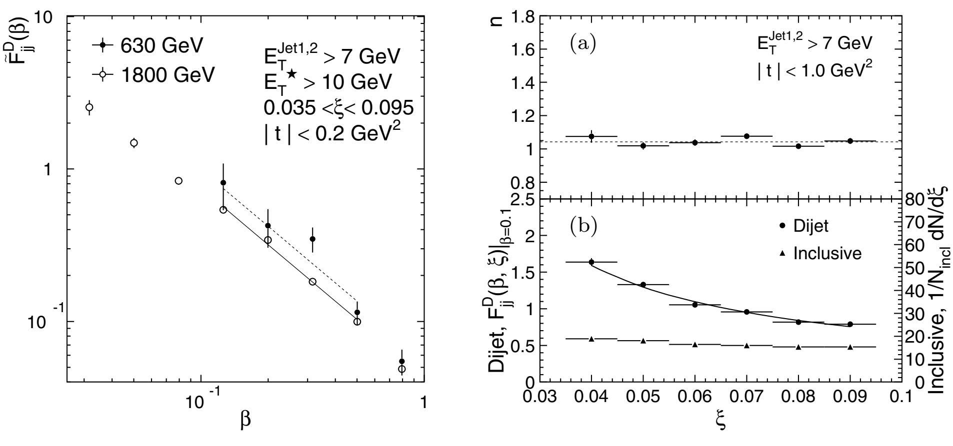

Fig. 13. (left) The diffractive structure function versus β, $\tilde{F}_{jj}^D(\beta)$, integrated over the range $0.035 < \xi < 0.095$ and $|t| < 0.2\,\text{GeV}^2$ and expressed per unit ξ, at $\sqrt{s} = 630\,\text{GeV}$ (black points) and 1800 GeV (open circles). The errors are statistical only. The lines are fits of the form β^{-n} with the parameter n common at both energies. In the fit region, the systematic uncertainty in the ratio of the 630 to 1800 GeV data is $^{+31}_{-23}\%$. (right) Distributions versus ξ for 1800 GeV data: (a) the parameter n of a fit to the diffractive structure function of the form $F_{jj}^D(\beta,\xi)|_\xi = C\beta^{-n}$ for $\beta < 0.5$; (b) the diffractive structure function at $\beta = 0.1$ fitted to the form $F_{jj}^D(\beta,\xi)|_{\beta=0.1} = C\xi^{-m}$ (circle-points and curve), and the inclusive single-diffractive distribution (triangles). The errors shown are statistical.

2.13. *III A* (13): *Diffractive W and Z production at the Fermilab Tevatron* (2010)[18]

This paper reports measurements of the fraction of events with a W or Z boson which are produced diffractively in $\bar{p}p$ collisions at $\sqrt{s} = 1.96\,\mathrm{TeV}$. The data used are from $0.6\,\mathrm{fb}^{-1}$ of integrated luminosity collected with the CDF II detector equipped with a RPS that detects the $\bar{p}$ from $\bar{p} + p \to \bar{p} + [X + W/Z]$. It is found that $(0.97 \pm 0.11)\%$ of Ws and $(0.85 \pm 0.22)\%$ of Zs are produced diffractively in a region of antiproton *or proton* fractional momentum loss ξ of $0.03 < \xi < 0.10$ and four-momentum transferred squared t of $-1 < t < 0$ $(\mathrm{GeV}/c)^2$. The events in which the proton scatters diffractively while the antiproton dissociates, $\bar{p} + p \to [X + W/Z] + p$, are accounted for by doubling the measured proton dissociation fraction. Also reported in this paper are searches for W and Z production in DPE, $p + \bar{p} \to p + [X + W/Z] + \bar{p}$, and for exclusive Z production, $\bar{p} + p \to \bar{p} + Z + p$. No signal is seen above background for either one of these two processes. The results are compared with theoretical expectations.

A schematic diagram of diffractive W and Z production is shown in Fig. 14. The main results are summarized in Fig. 15: on the left, the plot shows distributions of various datasets used for extracting the signal, while the plot on the right shows the W mass distribution extracted from the diffractive event sample.

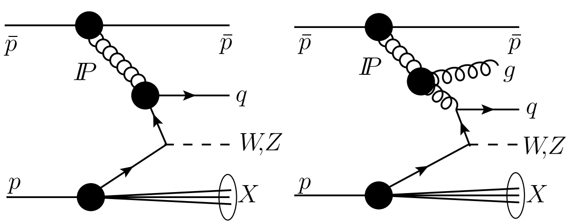

Fig. 14. Diffractive W production: (left) through quarks, and (right) through gluons.

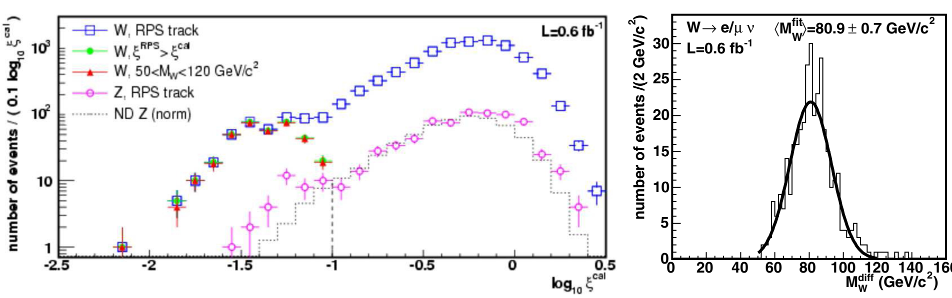

Fig. 15. (left) $\xi_{\bar{p}}^{\mathrm{cal}}$ for W and Z events with a RPS track; the dotted histogram is the distribution of nondiffractive (ND) Z events normalized to the data Z-distribution in the region $-1.0 < \log_{10}\xi_{\bar{p}}^{\mathrm{cal}} < -0.4$. (right) Reconstructed $M_{\mathrm{W}}^{\mathrm{diff}}$ with a Gaussian fit.

2.14. *III A* (14): *Diffractive dijet production in $\bar{p}p$ collisions at* $\sqrt{s} = 1.96\,\text{TeV}$ (2012)[19]

This paper reports results from a comprehensive study of diffractive dijet production in $\bar{p}p$ collisions at $\sqrt{s} = 1.96\,\text{TeV}$ using the CDF II detector at the Fermilab Tevatron $\bar{p}p$ collider. A data sample from 310 pb^{-1} of integrated luminosity collected by triggering on a high transverse energy jet, E_T^{jet}, in coincidence with a recoil antiproton detected in a RPS is used to measure the ratio of single-diffractive to inclusive-dijet event rates as a function of $x^{\bar{p}}$ of the interacting parton in the antiproton, the Bjorken-x ($x_{Bj}^{\bar{p}}$), and a $Q^2 \approx (E_T^{\text{jet}})^2$ in the ranges $10^{-3} < x_{Bj}^{\bar{p}} < 10^{-1}$ and $10^2 < Q^2 < 10^4\,\text{GeV}^2$, respectively. Results are presented for the region of $\bar{p}$-momentum-loss fraction $0.03 < \xi_{\bar{p}} < 0.09$ and a four-momentum transfer squared $t_{\bar{p}} > -4\,\text{GeV}^2$. The $t_{\bar{p}}$ dependence is measured as a function of Q^2 and $x_{Bj}^{\bar{p}}$ and compared with that of inclusive single diffraction dissociation. Only weak $x_{Bj}^{\bar{p}}$ and Q^2 dependencies in the ratio of single diffractive to inclusive event rates are found, and no significant Q^2 dependence in the diffractive $t_{\bar{p}}$ distributions.

This is in effect a measurement of the $\bar{p}$ diffractive structure function in $\bar{p}p$ collisions. The process is shown in Fig. 16. Special forward detectors are used, including a RPS, and a MiniPlug calorimeter: Fig. 17.

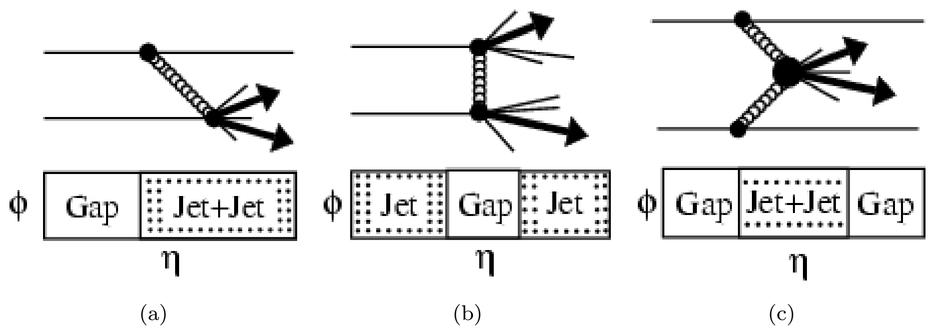

Fig. 16. Leading order schematic diagrams and event topologies in pseudorapidity (η) versus azimuthal angle (ϕ) for diffractive dijet production processes studied by CDF: (a) single diffraction, (b) double diffraction, and (c) DPE; the dot-filled rectangles represent regions where particle production occurs.

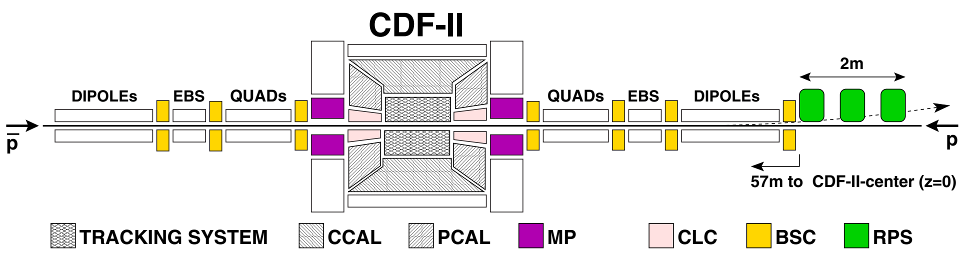

Fig. 17. Schematic plan view of the CDF II central (CDF-II) and forward detectors.

The main results are presented in Figs. 18 and 19. Figure 18 shows that the ratio of the diffractive to nondiffractive dijet event rates, which in LO is proportional to the ratio of the respective structure functions (NLO corrections are expected to be of $\mathcal{O}(10\%)$), varies by less than a factor of two over a Q^2 range of $\sim 10^3$ and Fig. 19 presents the $-t$ distribution, which is nearly independent of $\langle Q^2 \rangle$ over a wide range of $\langle Q^2 \rangle$ values.

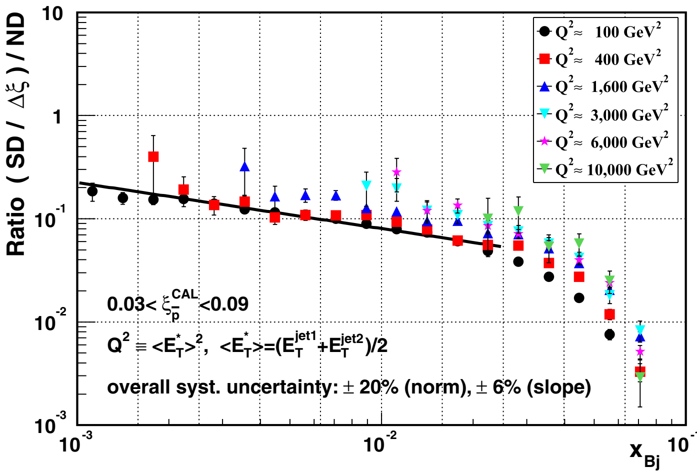

Fig. 18. The ratio of diffractive to nondiffractive dijet event rates as a function of x_{Bj} (momentum fraction of parton in the antiproton) for different values of $Q^2 \approx \langle E_T^* \rangle^2$. The quoted overall systematic uncertainty of $\pm 20\%$ is due to the uncertainties $\Delta\mathcal{R}_0$ and Δr listed in Table III.[19]

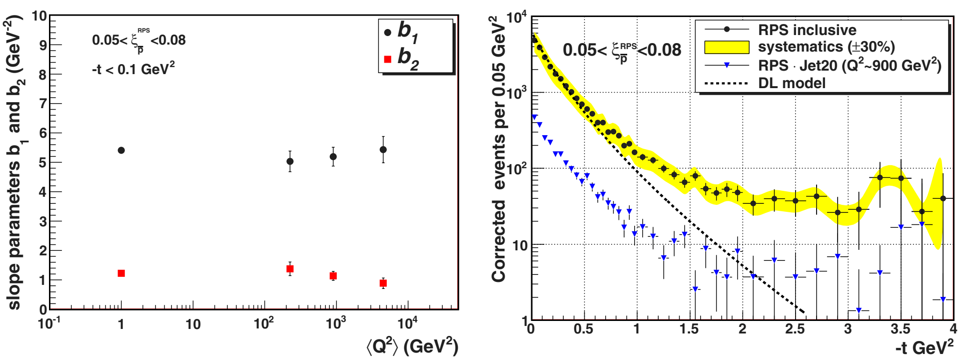

Fig. 19. (left) The slope parameters b_1 and b_2 of a fit to the form $d\sigma/dt = N \cdot (A_1 \cdot e^{b_1 \cdot t} + A_2 \cdot e^{b_2 \cdot t})$, with $A_2/A_1 = 0.11$ for SD events of different Q^2 values (right) t-distributions for two samples of SD $\mathrm{RPS}_{\mathrm{track}}$ events within the region $0.05 < \xi_{\overline{p}}^{\mathrm{RPS}} < 0.08$ corrected for RPS acceptance after background subtraction: (circles) RPS inclusive and (triangles) RPS $\cdot$ Jet20 ($\langle Q^2 \rangle \simeq 900\,\mathrm{GeV}^2$). The curve represents the distribution expected for soft SD in the DL (Donnachie–Landshoff) model [*Phys. Lett. B* **518**, 63 (2001], and references therein) normalized to the RPS data within $-t \lesssim 0.5\,\mathrm{GeV}^2$.

2.15. *III B* (15): *Dijet production by double pomeron exchange at the Fermilab Tevatron* (2000)[11]

This paper reports the first observation of dijet events with a DPE topology produced in $\bar{p}p$ collisions at $\sqrt{s} = 1800\,\mathrm{GeV}$. The events are characterized by a leading antiproton, two jets in the central pseudorapidity region, and a large rapidity gap on the outgoing proton side. Results are presented on jet kinematics and production rates, compared with corresponding results from single diffractive and inclusive dijet production, and tests of factorization are performed.

Process diagrams and results are presented in Figs. 20 and 21, respectively.

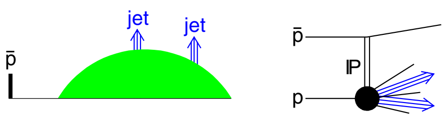

(a)

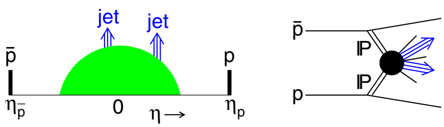

(b)

Fig. 20. Illustration of event topologies in pseudorapidity, η, and associated Pomeron-exchange diagrams for dijet production in (a) single diffraction and (b) DPE. The shaded areas on the left represent particles not associated with the jets (underlying event).

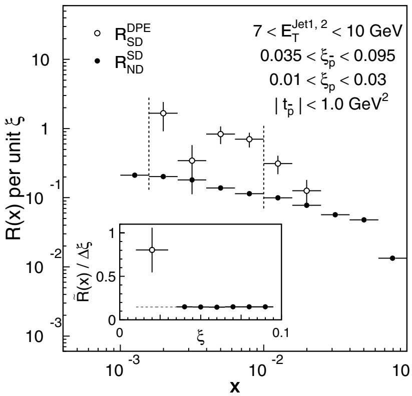

Fig. 21. Ratios of DPE to SD (SD to ND) dijet event rates per unit ξ_p ($\xi_{\bar{p}}$), shown as open (filled) circles, as a function x-Bjorken of partons in the p ($\bar{p}$). The errors are statistical only. The SD/ND ratio has a normalization systematic uncertainty of $\pm 20\%$. The insert shows $\tilde{R}(x)$ per unit ξ versus ξ, where the tilde over the R indicates the weighted average of the $R(x)$ points in the region of x within the vertical dashed lines, which mark the DPE kinematic boundary (left) and the value of $x = \xi_p^{\min}$ (right).

2.16. *III B* (16): *Observation of exclusive dijet production at the Fermilab Tevatron $p\bar{p}$ Collider* (2008)[17]

A mini-review of this paper appears in:
K. Goulianos, Central Exclusive dijet production at the Tevatron, *Int. J. Mod. Phys. A* (IJMPA), World Scientific Publishing Company.

Free access on-line publication: *https://arxiv.org/submit/1039825/view*
For completeness, the abstract of the above mini-review is copied below:

Abstract. We present a reference review of central exclusive dijet production in $\bar{p}p$ collisions, where the proton and antiproton emerge intact, and only two jets of transverse energy above a certain threshold are present in the final state. The results are published in two papers by the Collider Detector at Fermilab (CDF) Collaboration, a PRL (2000) and a PRD (2008), based on data collected at $\sqrt{s} = 1.8$ TeV and 1.96 TeV, respectively, and a D0 Collaboration paper from studies at 1.96 TeV. In all three cases predictions for the cross-section of Higgs boson production are discussed, a process that proceeds via a similar mechanism as dijet production. Roman Pot Spectrometers equipped with tracking detectors are used to measure the outgoing antiproton (CDF and D0) and proton (D0), and special forward detectors are employed to help reduce backgrounds and enrich the data in diffractive and exclusive dijet events.

2.17. *III C* (17): *Observation of rapidity gaps in $\bar{p}p$ collisions at* 1.8 TeV (1995)[4]

In $p\bar{p}$ collisions at $\sqrt{s} = 1.8$ TeV jet events are found with a rapidity gap topology. The number of hadrons in the rapidity interval $\Delta\eta_D$ between leading-jet cones is sampled by charged tracks with $P_T > 100\,\mathrm{MeV}/c$. An excess of trackless events beyond that expected in a smooth multiplicity distribution is observed. In a control region outside $\Delta\eta_D$ no excess is seen. For $\Delta\eta_D > 0.8$, the fraction of excess trackless events, consistent with estimates based on exchange of color-singlet digluons, is $R(\text{gap}) = \frac{\sigma_{\text{jet}}(\text{gap})}{\sigma_{\text{jet}}} = 0.0085 \pm 0.012\,(\text{stat})^{+0.0024}_{-0.0012}\,(\text{syst})$.

The signal is extracted by fitting data in the η-region between the jets (G) and the "background" regions that contain the jets (N), Fig. 22.

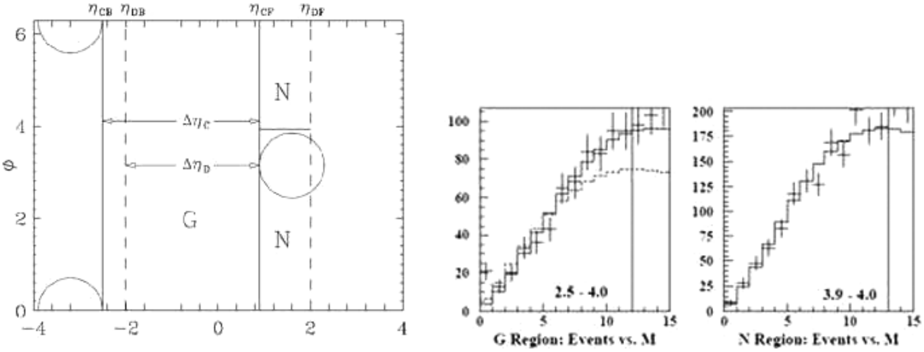

Fig. 22. (left) ϕ versus η phase space, and (right) (a) gap and (b) no-gap regions.

2.18. *III C* (18): *Dijet production by color-singlet exchange at the Fermilab Tevatron* (1998)[7]

This paper reports a new measurement of dijet production by color-singlet exchange in $p\bar{p}$ collisions at $\sqrt{s} = 1.8\,\text{TeV}$ at the Fermilab Tevatron. In a sample of events with two jets of transverse energy $E_T^{\text{jet}} > 20\,\text{GeV}$, pseudorapidity in the range $1.8 < |\eta^{\text{jet}}| < 3.5$, and $\eta_1\eta_2 < 0$, it is found that a fraction $R = 1.13 \pm 0.12\,(\text{stat}) \pm 0.11\,(\text{syst})\%$ have a pseudorapidity gap within $|\eta| < 1$ between the jets that can be attributed to color-singlet exchange. The fraction R shows no significant dependence on E_T^{jet} or on the pseudorapidity separation between the jets.

The color-singlet signal is extracted using events with jets on opposite sides of the $|\eta| < 1.0$ region from the correlation of calorimeter towers versus tracks, as shown in Fig. 23 (left). The signal is contained mostly in the region of events with zero-tracks and less than three calorimeter towers. In Fig. 23(c), the ratio of gap to control-sample no-gap events (normalized to be unity on average) is plotted versus 1/2 of the η separation between the jets. It is seen that the gap signal becomes increasingly more dominant as $|\eta_1 - \eta_2|/2$ increases.

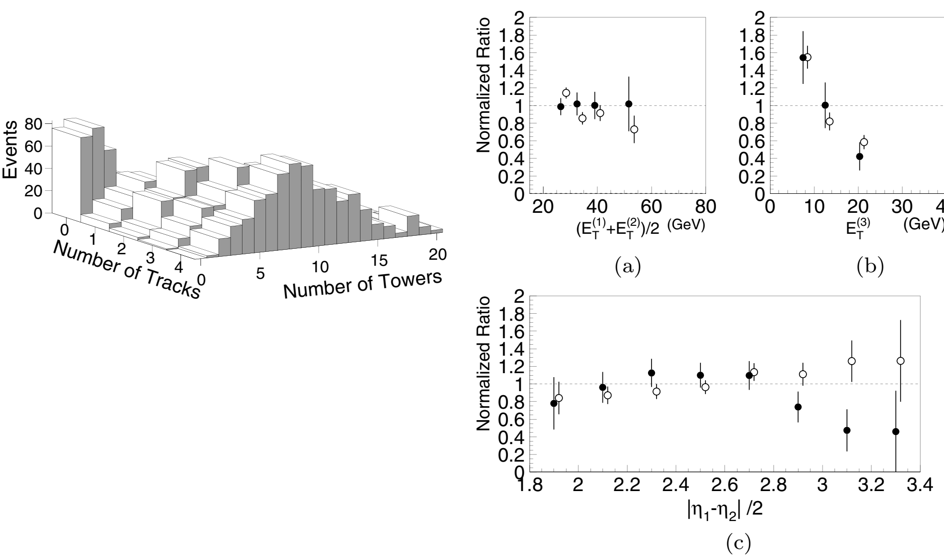

Fig. 23. (left) Track versus tower multiplicity distribution for events in the $N_{\text{vertex}} \leq 1$ opposite-side dijet sample with $N_{\text{track}} < 5$ and $N_{\text{tower}} < 20$ within $|\eta| < 1.0$. The bins with zero tracks and 0, 1 or 2 towers contain an excess of events above the expectation from an extrapolation from the bins with $N_{\text{track}} > 1$. This excess is attributed to events from color-singlet exchange. (right) Normalized (to be unity on average) ratios of gap (solid points) and control sample events (open circles) over all events versus: (a) the average E_T of the two leading jets, (b) the E_T of the third jet, and (c) half the η separation between the two leading jets.

2.19. *III C* (19): *Events with a rapidity gap between jets in $\bar{p}p$ collisions at* $\sqrt{s} = 630\,\text{GeV}$ (1998)

This paper reports a measurement of the fraction of dijet events with a rapidity gap between jets produced by a color-singlet exchange in $\bar{p}p$ collisions at $\sqrt{s} = 630\,\text{GeV}$ at the Fermilab Tevatron. In events with two jets of transverse energy $E_T^{\text{jet}} > 8$ GeV, pseudorapidity in the range $1.8 < |\eta^{\text{jet}}| < 3.5$, and $\eta_1\eta_2 < 0$, the color-singlet exchange fraction is found to be $R = [2.7 \pm 0.7\,(\text{stat}) \pm 0.6\,(\text{syst})]\%$. Comparisons are made with results obtained at $\sqrt{s} = 1800\,\text{GeV}$ and with theoretical expectations.

The color-singlet exchange signal is extracted by comparing the track and calorimeter tower multiplicity distributions for opposite-side (OS, $\eta_1\eta_2 < 0$) dijet events, which are rich in signal, and same-side ones (SS, $\eta_1\eta_2 > 0$), which are dominated by nondiffractive events. The ratio of OS to SS events, normalized to the SS ones, is plotted in Fig. 24 versus the number of tracks (left) and towers (right). A clear signal is seen in both cases in the regions of $N_{\text{track}} > 0$ and $N_{\text{tower}} < 3$, respectively.

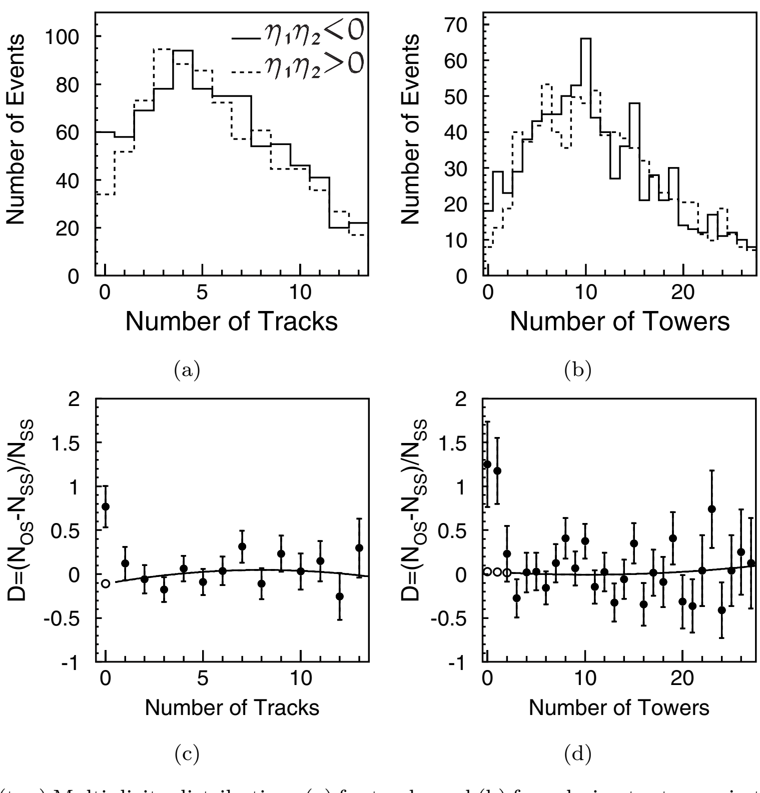

Fig. 24. (top) Multiplicity distributions (a) for tracks and (b) for calorimeter towers in the regions $|\eta| < 0.9$ for opposite-side (OS, $\eta_1\eta_2 < 0$) dijet events (solid lines), and $|\eta| < 1.05$ ($|\eta| < 1.2$) for tracks (towers) for same-side (SS, $\eta_1\eta_2 > 0$) dijet events (dashed lines); (bottom) the bin-by-bin difference between OS and SS events normalized to the number of SS events. The SS distribution is scaled to the OS one by the ratio of OS/SS events for $N_{\text{track}} > 0$ in (a) and $N_{\text{tower}} > 2$ in (b).

Acknowledgments

I would like to thank my CDF colleagues for their contributions that made this work possible, and the Office of Science of the Department of Energy and the Rockefeller University for their generous financial support.

References

1. CDF Collab., (F. Abe *et al.*), *Phys. Rev. D* **50**, 5518 (1994).
2. CDF Collab. (F. Abe *et al.*), *Phys. Rev. D* **50**, 5550 (1994).
3. CDF Collab. (F. Abe *et al.*), *Phys. Rev D* **50**, 5535 (1994).
4. CDF Collab. (F. Abe *et al.*), *Phys. Rev. Lett.* **74**, 855 (1995).
5. CDF Collab. (F. Abe *et al.*), *Phys. Rev. Lett.* **78**, 2698 (1997).
6. CDF Collab. (F. Abe *et al.*), *Phys. Rev. Lett.* **79**, 2636 (1997).
7. CDF Collab. (F. Abe *et al.*), *Phys. Rev. Lett.* **80**, 1156 (1998).
8. CDF Collab. (F. Abe *et al.*), *Phys. Rev. Lett.* **81**, 5278 (1998).
9. CDF Collab. (T. Affolder *et al.*), *Phys. Rev. Lett.* **84**, 232 (2000).
10. CDF Collab. (T. Affolder *et al.*), *Phys. Rev. Lett.* **84**, 5043 (2000).
11. CDF Collab. (T. Affolder *et al.*), *Phys. Rev. Lett.* **85**, 4215 (2000).
12. CDF Collab. (T. Affolder *et al.*), *Phys. Rev. Lett.* **87**, 141802 (2001).
13. CDF Collab. (T. Affolder *et al.*), *Phys. Rev. Lett.* **87**, 241802 (2001).
14. CDF Collab. (D. Acosta *et al.*), *Phys. Rev. Lett.* **88**, 151802 (2002).
15. CDF Collab. (D. Acosta *et al.*), *Phys. Rev. Lett.* **91**, 011802 (2003).
16. CDF Collab. (D. Acosta *et al.*), *Phys. Rev. Lett.* **93**, 141601 (2004).
17. CDF Collab. (T. Aaltonen *et al.*), *Phys. Rev. D* **77**, 052004 (2008).
18. CDF Collab. (T. Aaltonen *et al.*), *Phys. Rev. D* **82**, 112004 (2010).
19. CDF Collab. (T. Aaltonen *et al.*), *Phys. Rev. D* **86**, 032009 (2012).